ELSEVIER

Ceramics International 31 (2005) 315–321

CERAMICS INTERNATIONAL

www.elsevier.com/locate/ceramint

Dielectric properties of plasma-sprayed silicates

Pavel Ctibor[a,*], Josef Sedláček[b], Karel Neufuss[a], Jiří Dubský[a], Pavel Chráska[a]

[a] *Materials Engineering Department, Institute of Plasma, Physics Academy of Sciences of the Czech Republic, 182 21 Prague 8, Czech Republic*

[b] *Department of Mechanics and Materials Science, Faculty of Electrical Engineering, Czech Technical University, 166 27 Prague 6, Czech Republic*

Received 16 April 2004; received in revised form 5 May 2004; accepted 15 May 2004
Available online 25 August 2004

Abstract

Several silicate materials were plasma sprayed and characterized by the authors in recent years from the point of view of their sprayability, chemical and phase compositions, microstructure and mechanical as well as thermal properties. Present work is concerned with selected dielectric properties of these deposits.

Synthetic mullite, steatite and spodumene as well as natural olivine–forsterite were plasma sprayed using the water-stabilized plasma system (WSP®). The deposits were striped-out, ground and polished to produce samples in a shape of planparallel plates with a smooth surface. These samples—in principle monoblock capacitors—were then tested in the alternative low voltage electric field to measure capacity and loss factor in the frequency range from 200 Hz to 1 MHz. Relative permittivity was calculated from the measured capacity. Volume resistivity was measured in the direct electric field. In addition dielectric strength of steatite was measured at 50 Hz ac. It is shown that the relative permittivity of plasma-sprayed silicates is less stable compared to bulk in the whole studied frequency range. Insulating ability of plasma-sprayed silicates is discussed in comparison with the bulk ceramics with the same composition. Paths of the electrical breakdown of plasma-sprayed steatite are observed by microscopy to help to resolve the failure mechanism.

Keywords: B. Optical microscopy; C. Electrical properties; D. Silicates; E. Insulators; Plasma spraying

1. Introduction

The family of SiO_2-based ceramics is widely used in electrical industry, especially as insulators. Sintered silicates exhibit excellent volume resistivity and minimal dielectric losses under a wide range of conditions. These two parameters are strongly connected together and they also reflect the material structural features such as the crystallinity and grain size.

In recent years at the Institute of Plasma Physics (IPP) large number of silicates was examined from the point of view of ability to be successfully processed by the water-stabilized plasma system (WSP®). Resulting deposits were studied to gain basic characterization of such materials and found and evaluate differences in structure and properties induced by plasma spraying process in comparison to conventional furnace processes used in ceramic industry. The group of silicates is wide and important and therefore it is necessary to carry out experiments on many different compositions before successful generalizations could be made. Present work is only a small piece in such a mosaic.

After successful spraying of zircon [1] the IPP group has continued in looking for inexpensive natural silicate materials prospective for spraying. Garnets [2] were successfully applied, but their composition is too complicated and some structural features of deposits so extraordinary that IPP decided to continue with more simple chemical compositions in following work. Synthetic silicates: wollastonite, mullite, cordierite and steatite were tested and the first results referred [3]. After their spraying more detailed study of them started and in the same time spraying of other silicates was performed. We followed both above-mentioned ways of

* Corresponding author. Tel.: +420 2 6605 3727; fax: +420 2 8658 6389.
E-mail address: ctibor@ipp.cas.cz (P. Ctibor).

0272-8842/$30.00
doi:10.1016/j.ceramint.2004.05.022

searching—for inexpensive natural, but relatively simple, materials and for materials complementary with earlier tested synthetic (fused feedstock-based) oxide deposits. This recent series of experiments includes natural olivine–forsterite, synthetic spodumene and several SiO_2-based glassy compositions. Although, comprehensive report of their plasma spraying is not in focus of this paper.

The authors move subsequently to chemical compositions with lower melting points, especially in the system $MgO–Al_2O_3–SiO_2$ (see equilibrium diagram in Fig. 1, precisely described in [4]), which is in present time almost completely covered by spraying experiments done at IPP. Previous extensive results were gained for Al_2O_3, e.g. [5], and also several interesting but rather disputable results were obtained for MgO [6]. But the papers [5,6] were focused only on end members of this ternary system, which were studied as fused feedstock-based oxide deposits.

In present work, we are focused on synthetic mullite $3Al_2O_3–2SiO_2$—pure and also in mechanical mixture with 15 wt.% of glass, steatite $MgSiO_3$ and spodumene $Li_2O–Al_2O_3–4SiO_2$ as well as on natural olivine having near-forsterite (Mg_2SiO_4) composition. All these materials are frequently used in electric industry. *Mullite* is a material undergoing no transformation in solid state and it is a refractory [7]. It exhibits perfect stability of dimensions during thermal cycling [8]. Its use in electrical industry is limited to mechanically supporting parts due to its high loss factor [9]. *Steatite* is used in high-frequency devices (as coil cores, supporting parts of switches and insulations in general) thanks to its low loss factor and good mechanical properties [10]. *Spodumene* is useful in the same way as mullite. It has extremely low thermal expansion and therefore it could serve as supporting part for high variety of conductive materials. On the other hand, *forsterite* has a very high thermal expansion coefficient. It is frequently used in the same way as steatite in electric industry as insulation, but especially in vacuum devices where forsterite and its high thermal expansion coefficient is utilized in combination with metallic parts. Loss factor of forsterite is low and independent on frequency [10].

Above-mentioned character of each of these materials in commercial bulk form is obtained thanks to their small grain

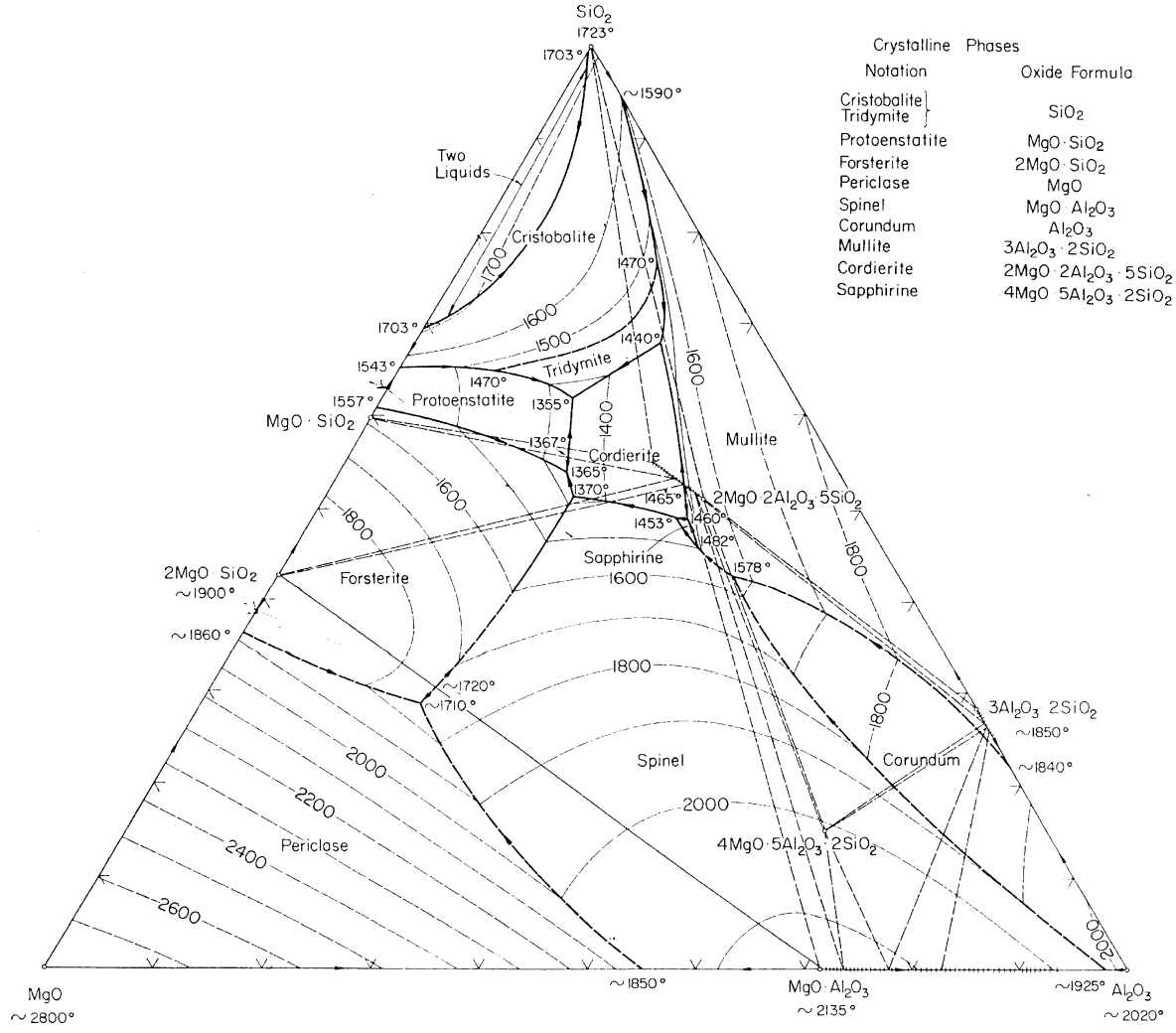

Fig. 1. Phase diagram of the system $MgO–Al_2O_3–SiO_2$ [4].

sizes, low and uniformly distributed closed porosity and moreover thanks to a relatively low glassy phase content. Classical furnace processes like sintering or manufacturing of glass–ceramics [7,8] lead to production of the above-described structures.

All synthetic materials were obtained in the form of tablets of industrial purity, produced by the sintering or reactive sintering of previously calcinated powder. Natural forsterite was in the form of raw mineral, received as blocky pieces. All materials were crushed and sieved to obtain feedstock powder for spraying (size 63–125 μm). It is necessary to point out that they include (with exception of natural forsterite) a certain amount of alkali or other metallic impurities due to the previous fabrication of the tablets. In addition, Fe content in the powders has increased also due to wear of steel parts of crushing apparatus.

2. Experimental

2.1. Plasma spraying

Mullite and steatite were selected from silicate deposits described in [3] as materials having lowest open as well as total porosity. Mullite was sprayed using shorter stand-off distance, SD, than in [3] (300 mm instead of 350 mm) and metallic titanium as substrate material was used.

The samples were manufactured using high-throughput water-stabilized plasma spray system WSP® PAL 160 (IPP, Prague, Czech Republic). This system operates at about 160 kW arc power and can process high amounts of material per hour. In the current experiment feedstock throughputs of 22–24 kg/h were used, i.e., about 50% of maximum available throughput of this system. Main spray parameters of this system—feeding distance and spray distance—were optimized by checking single splats shapes and sizes before deposition. Optimum preheating temperature of the substrate was also found from the splats shape. Spray distances used (SD) were 350, 450 and 550 mm [3]. As substrates carbon steel (AISI 1016) as well as stainless steel (AISI 316) coupons were used. The powder was fed in by compressed air through two injectors. Deposited thickness was about 2.5 mm. The deposits were then stripped from the substrate by releasing agent or by thermal cycling at approximately ±100 °C to form self-supporting ceramic samples.

3. Measurements

3.1. Specimen preparation

The stripped-off ceramic samples were then ground from both sides to produce planparallel plates with a smooth surface. Such specimens represent in principle monoblock capacitors with dimensions 10 mm × 10 mm × 1 mm. A thin layer of aluminum as the electrode plates from both sides was sputtered in reduced pressure (2×10^{-3} Pa) on the ground surface. Samples for electric strength measurement were ground without subsequent sputtering of metallic contacts.

3.2. Description of the electric measurements

Electric measurements were carried out at the CTU in Prague, Faculty of Electrical Engineering, Department of Mechanics and Materials Science, Czech Republic. The electric field was applied parallel to the spraying direction (i.e., perpendicular to the substrate surface).

Capacity was measured in the frequency range from 200 Hz to 1 MHz using programmable LCR-meter (PM 6306, Fluke, USA). The frequency step was 100 Hz between 200 and 1000 Hz, 1 kHz between 1 and 10 kHz, 10 kHz between 10 and 100 kHz, and 100 kHz between 100 kHz and 1 MHz. Test signal voltage was 1 V ac, the stabilized electric LCR-meter was equipped with a micrometric capacitor as recommended in the relevant standard [11]. Relative permittivity ε_r was calculated from measured capacities and specimen dimensions.

This same LCR-meter (PM 6306) was used for the loss factor measurement. Loss factor tg δ was measured at the same frequencies as capacity.

Electric resistance was measured with a special resistivity adapter—Keithley model 6105. The electric field was applied from a regulated high-voltage source and the values read by a multi-purpose electrometer (617C, Keithley Instruments, USA). The magnitude of the applied voltage was 100 ± 2 V dc. Volume resistivity was calculated from the measured resistance and specimen dimensions. In averages four to five specimens were measured and the average calculated.

Breakdown voltage was measured on the self-made apparatus (Department of Electrotechnology, Faculty of Electrical Engineering CTU, Prague) convenienced to the relevant standard [12]. Continuous increase of the applied voltage at 50 Hz ac (ambient atmosphere, room temperature) was maintained until breakdown or flashover occurs. Dielectric strength was calculated from breakdown voltage and specimen thickness. Five specimens of each material state were tested.

3.3. Porosity characterization

Porosity was studied by optical microscopy on polished cross-sections. Micrographs were taken via CCD camera and processed using the image analysis (IA) software (Lucia D, Laboratory Imaging, Czech Rep.). Minimum 10 images of microstructures, taken from various areas of a cross-section for each sample, were analyzed.

3.4. Phase composition

Phase analysis was done by X-ray diffraction (XRD, diffractometer D 500, Siemens, Germany) using the filtered Cu K_α radiation in the diffraction angle interval from 5 to 90° 2θ.

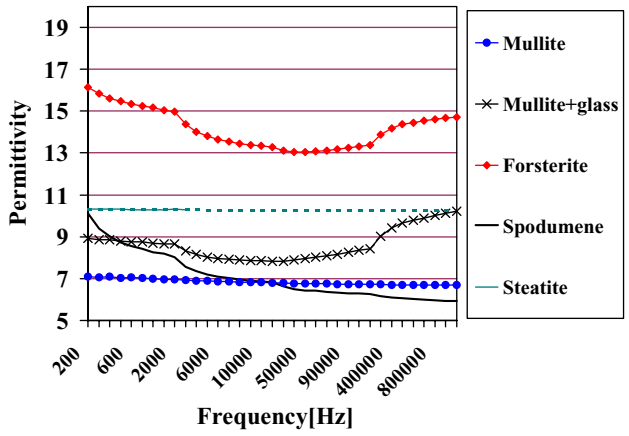

Fig. 2. Frequency dependence of relative permittivity (from 200 to 10^6 Hz).

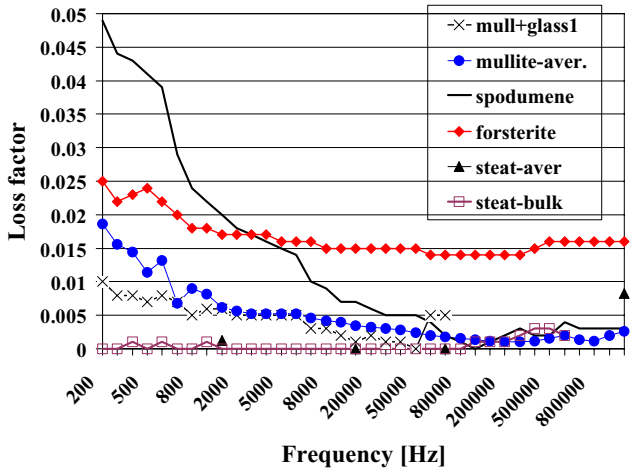

Fig. 3. Frequency dependence of loss factor (from 200 to 10^6 Hz). Steat-aver means plasma deposit.

Table 1
Comparison between relative permittivity of plasma deposits and literary values of bulk analogs at frequency 1 MHz

Material	Permitivity	
	Plasma sprayed	Bulk
Mullite	6.7	4 [9]
Mullite + 15% glass	10.2	n.a.
Olivine–forsterite	14.7	6–8.5 [10]
Spodumene	6.0	10.4 [4], frequency n.a.
Steatite	10.3	6 [9]

Corresponding reference is added in brackets.

Table 2
Comparison between loss factor of plasma deposits and literature values of bulk analogs at frequency 1 MHz

Material	Loss factor	
	Plasma sprayed	Bulk
Mullite	2.6×10^{-3}	1.6×10^{-2} [9]
Mullite + 15% glass	5×10^{-3} at 70 kHz	n.a.
Olivine–forsterite	1.6×10^{-2}	4×10^{-4} [8]
Spodumene	3×10^{-3}	n.a.
Steatite	8.3×10^{-3}	1.5-2 $\times 10^{-3}$ [13]

Corresponding reference is added in brackets.

4. Results

4.1. Permittivity

Relative permittivity results are shown in Fig. 2. In general, plasma deposits have slightly higher permittivity than the bulk ceramics, as can be seen in Table 1.

4.2. Loss factor

Measured values of the loss factor are summarized in Fig. 3 and reference values for bulk ceramics are given in Table 2. Losses in plasma-sprayed materials are in general those of the bulk. Loss factor of plasma deposits (except forsterite, which is in agreement with literature [10]) exhibits certain decrease with increasing frequency. This is also typical for bulk ceramics [14,16].

4.3. Volume resistivity

The resistivity results are summarized in Table 3. Plasma deposits have resistivity in a very wide range. On one side, values for mullite and mullite–glass mixture are comparable with bulk material. On the other side, steatite and spodumene deposits show values approximately 4 orders of magnitude lower than that of the bulk.

Table 3
Volume resistivity of plasma deposits and bulk analogs, porosity of plasma deposits

Material	Resistivity (Ωm)		Porosity of plasma deposits (%)
	Plasma sprayed	Bulk[a]	
Mullite	5.34×10^{10}	10^{10} [9] to 10^{11}	7.8
Mullite + 15% glass	2.28×10^{10}	n.a.	4.2
Olivine–forsterite	3.87×10^{9}	10^{11}	4.4
Spodumene	1.99×10^{9}	5×10^{11} [10]	n.a.
Steatite	8.09×10^{6}	10^{11}	3.7

[a] Values without reference in brackets were measured by the authors.

Table 4
Dielectric strength of steatite plasma deposits and bulk analogs

Material state	Dielectric strength (kV/mm)	Standard deviation (kV/mm)
Plasma sprayed	3.41	0.31
Bulk	10.34	0.73

4.4. Dielectric strength

In Table 4 average values as well as standard deviations are summarized. The value at bulk should be considered as minimum, because at two specimens only flashover occurs until maximum of available voltage was reached. The delay on maximum voltage was limited to maximum 30 s to avoid cumulating of heat in the specimen induced by time factor.

5. Discussion

5.1. Influence of porosity, phase composition and chemical purity on permittivity

The difference between the deposit's and the bulk's permittivity values could be accounted for through a combination of at the minimum two effects. One of them is the presence of moisture absorbed within the voids [15]. We could perform calculations of the relative permittivity of the deposit as two-component system ε_v (ceramics and voids) according to, for example, Lichtenecker logarithmic formula [16].

$$\log \varepsilon_v = v_i \log \varepsilon_i + v_e \log \varepsilon_e$$

Let v_i be the volume of ceramics, ε_i the relative permittivity of ideal void-free bulk ceramics (so called 'intrinsic permittivity'), v_e the total volume of voids (obtained by image analysis, see Table 3) and ε_e the relative permittivity of water—as the extreme case of medium filling the voids.

However, results presented in Table 5, show that moisture in voids cannot itself explain the measured results in Table 1. If we bear in mind the method of the bulk silicates fabrication, it is evident that first of all the presence and amount of the amorphous phase controls the relative permittivity of silicates [10]. In Fig. 2 we can see a certain relaxation (i.e., decrease with growing frequency) of permittivity. This corresponds to the fact, that in bulk silicates the relaxation is caused by alkali ions in the amorphous phase, which could shift itself in the electric field and contribute to the polarization [16]. The higher the amount of amorphous phase in the material, the higher the polarization and therefore the permittivity (for deeper discussion see [17,18]). If we focus on the phase composition of our deposits, we see, that amorphous phase is dominant in the deposits. Steatite deposits are completely amorphous and mullite dominantly amorphous with traces of crystalline mullite and gamma alumina [3]. Crystalline spodumene feedstock was converted to amorphous after spraying, when quartz was observed as crystalline phase in both states. Fully crystalline forsterite feedstock was also amorphized, only traces of original Mg_2SiO_4 phase (PDF 34-189) remained in the deposit.

Table 5
Relative permittivity calculated according to Lichtenecker logarithmic formula

Material	v_e	ε_e	v_i	ε_i	ε_v
Forsterite-minimum	0.044	90	0.956	6	6.76
Forsterite-maximum	0.044	90	0.956	8.5	9.43
Mullite + glass	0.042	90	0.958	4	4.56
Mullite-minimum	0.078	90	0.922	4	5.10
Mullite-maximum	0.078	90	0.922	6.6	8.09
Steatite	0.037	90	0.963	6.5	7.16

Under 'minimum' and 'maximum' the extreme values of ε_i found in the literature are considered in calculation.

The amorphization of originally crystalline feedstock, see also [3], during the spraying process is probably associated with very narrow interval between solidus and liquidus in these materials (approximately 40 K at steatite, only few K for spodumene [16]).

Chemical composition investigation by X-ray fluorescence analysis method proved, that impurities like K, Ca, Ti and Fe were present in the feedstock. In deposits their content decreases but certain amount remains in all materials. The increase of relative permittivity of forsterite and mullite-glass mixture above approximately 40 kHz is so far not well understood.

5.2. Loss factor as indication of polarizing mechanisms

Dielectric losses represent the portion of the electric field energy dissipated to heat in the ceramic body. In Fig. 3 it is visible that spodumene—the same material, which exhibits the highest relaxation of permittivity, exhibits also the most impressive frequency dependence of the loss factor. But the other deposits have also similar character of losses. It indicates, that the ions shifted by the ac field consume for this movement a certain energy. This phenomenon is well pronounced at low frequencies. At higher frequencies, where the fast changes of the field direction enables the shift in limited extend only, the loss factor decreases. The part of the polarization, which is associated with these ions, disappears. At 1 MHz, and above, the polarization of the void-filing medium or other frequency-independent mechanisms are dominant.

5.3. Volume resistivity—influence of impurities

The resistivity results, Table 3, show that mullite and mullite–glass mixture have excellent resistivity—the same as bulk material. In the case of forsterite and spodumene there is a certain difference between plasma sprayed and bulk ceramics and finally plasma-sprayed steatite has insufficient resistivity. The authors suppose that in steatite ionic conductivity via the transport of present impurities must be activated. Steatite deposits and more or less also the others, see figures in

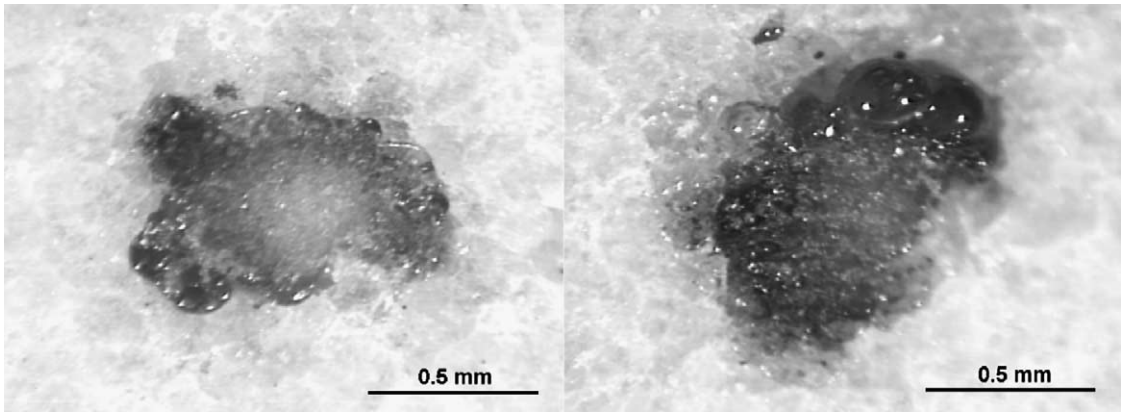

Fig. 4. Top-side (left) and bottom-side (right) of steatite plasma deposit after breakdown; light microscopy. On the bottom-side bubbles inside the remelted channel are visible.

[3], exhibits a special kind of microstructure without any splats, flat pores and cracks. Such a structure represents 'barrier-free' environment for transport of impurities.

The difference in resistivity between steatite plasma deposits and bulk steatite increases with voltage as will be documented in the following paragraph.

5.4. Dielectric strength

The results obtained at high voltage on the steatite deposits supports the conclusion of the previous paragraph. The difference in resistivity between plasma deposits and bulk is well pronounced also at high voltage. The average dielectric strength value of plasma-sprayed steatite is only one third of the bulk value. The character of the breakdown channel (Fig. 4) confirms, that rapid melting of the ceramic body occurs directly before breakdown. Here the resistance locally decreases and enables cumulating of the charge until short-circuit is completed through the specimen thickness. At the short-circuit, current of 20–30 mA flows through the specimen. The same character of the behavior in the strong electric field is also typical for bulk steatite, see Fig. 5—also here the volume remelted at flashover contains several large bubbles (approximately 0.1 mm).

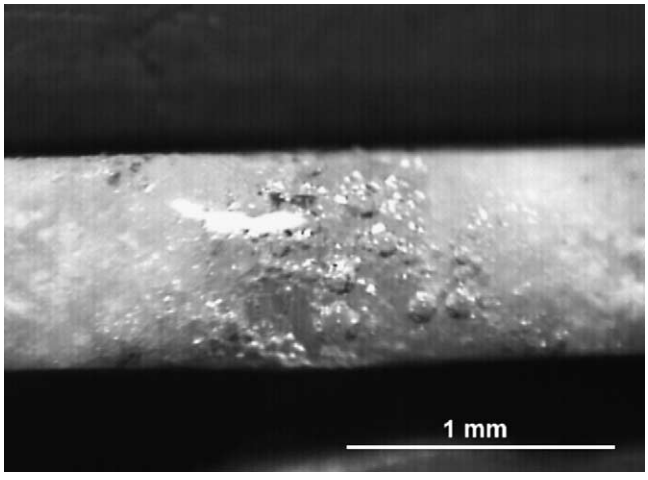

Fig. 5. Edge of the bulk steatite specimen after flashover at dielectric strength measurement. The central, approximately 1 mm wide, part is remelted at flashover and contains big bubbles.

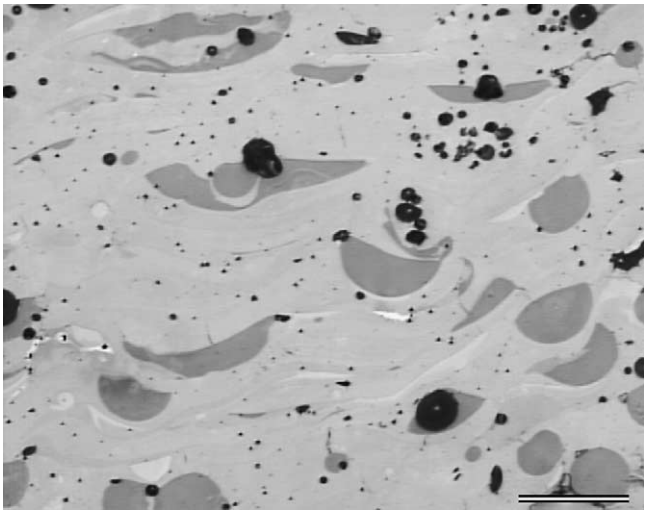

Fig. 6. Plasma deposit made from the feedstock prepared as mechanical mixture of mullite with 15 wt.% of glass. Light microscopy, polished cross-section, length of the bar is 100 μm.

5.5. Structure

The same structural features as described in [3] were found in our samples. Interesting is especially the mixture of mullite and glass, which forms a composite structure (Fig. 6).

6. Conclusions

Quality of deposits manufactured by plasma spraying could be examined from various points of view. Present work is concentrated on their dielectric properties. Plasma deposits exhibit several differences compare to bulk. Relative permittivity is in general higher than at bulk and more frequency-dependent. On the other hand also the loss factor of the deposits is higher and strongly frequency-dependent

in majority of studied deposits. Volume resistivity of majority of studied plasma deposits is lower than that of the bulk analogs. It has been found that the phase composition and the presence of impurities can markedly affect the resulting values while the porosity's influence is ambiguous. The insufficiency of plasma-sprayed steatite as insulator is supported also with electric strength measurement. Thermal character of the breakdown, which is typical for bulk steatite as well, develops in the plasma-deposited material at significantly lower voltage than at bulk. Other materials were not measured yet.

Annealing of as-sprayed deposits and their study in the annealed state is an interesting way of future experimental activities because their low crystallization temperatures. This fact suggests that annealing of these coatings can be done at metallic substrates without a serious damage of the metals. Especially the forsterite is a good prospective from this point of view. Spraying of materials with dominant amount of silica is a challenge for completely different set-up of needed parameters.

Acknowledgments

This work was supported by the Grant Agency of the Czech Republic under No. 202/03/0708. The authors thank to J. Petr, FEE CTU, for measurement of electric breakdown and to B. Kolman from IPP ASCR for valuable consultations.

References

[1] P. Chráska, K. Neufuss, H. Herman, Plasma spraying of zircon, J. Thermal Spray Technol. 6 (4) (1997) 445–448.
[2] K. Neufuss, B. Kolman, P. Chráska, J. Dubský, Plasma spraying of silicates, in: C. Berndt (Ed.), in: Proceedings of ITSC 98, 1998, pp. 636–640.
[3] K. Neufuss, J. Ilavsky, J. Dubsky, B. Kolman, P. Chraska, Plasma spraying of silicates II, in: Proceedings of the United Thermal Spray Conference 99, Dusseldorf, Germany, 1999, pp. 636–640.
[4] W. Hinz, Silikate—Basics of the Science and Technology, Berlin, 1970 (in German).
[5] P. Chráska, J. Dubský, K. Neufuss, J. Písačka, Alumina-base plasma-sprayed materials—part I: phase stability of alumina and alumina–chromia, J. Thermal Spray Technol. 6 (3) (1997) 320–326.
[6] K. Neufuss, et al., APS spraying of MgO and CeO_2 with WSP, in: Proceedings of 14th International Symposium on Plasma Chemistry, Prague, Czech Republic, 1999, pp. 2075–2079.
[7] Z. Strnad, Glassy-Crystalline Materials, Praha, 1983 (in Czech).
[8] J. Hlaváč, Basic of the Silicates Technology, Praha, 1988 (in Czech).
[9] F. Singer, S. Singer, Industrial Ceramics, 3th Band—The Ceramic Products, Berlin, 1966 (in German).
[10] Z. Pospíšil, A. Koller et al., Fine Ceramics—1st Band, Praha, 1981 (in Czech).
[11] Czech Standard ČSN IEC 250, Czech Institute for Standardization, 1997 (in Czech).
[12] Czech Standard ČSN EN 60243-1 (IEC 60243-1:1998), Czech Institute for Standardization, 1999 (in Czech).
[13] H. Sholze, The Physical and Chemical Basics of Ceramics, Berlin, 1968 (in German).
[14] H. Landolt, R. Boernstein, Values and Functions in Physics, Chemistry, Astronomy, Geophysics and Technology, Part 3, vol. IV, Springer Verlag, Berlin, 1957 (in German).
[15] L. Pawlowski, The relationship between structure and dielectric properties in plasma-sprayed alumina coatings, Surf. Coat. Technol. 35 (1988) 285–298.
[16] A. Koller, Structure and Properties of Ceramics, Elsevier, New York, 1994.
[17] H. Insley, V.D. Frechette, Microscopy of Ceramics and Cements, New York, 1955.
[18] N.E. Hill, Dielectric Properties and Molecular Behavior, Van Nostrand–Reinhold, London, 1969.